

GNN Interpretability Using Bayesian Inference

Shalin Patel

Advisor: Dr. Ritambhara Singh
Second Reader: Dr. Lorin Crawford



Division of Applied Mathematics and Department of Computer Science

Brown University

2023-04-18

Contents

1	Introduction	3
1.1	Graph Neural Networks	3
1.2	Interpretation on GNNs	5
1.3	Bayesian Inference	6
1.3.1	Stochastic Variational Inference (SVI)	7
1.3.2	Bayes-by-backprop	9
1.4	Normalizing Flows	9
2	Related Work	11
2.1	GNN Explainer	11
2.1.1	Benchmark Datasets	12
2.2	Parametrized-Graph Explainer	15
2.3	Other Explainer Frameworks	17
2.3.1	SubgraphX	17
2.3.2	GEM	18
2.4	SERGIO	18
3	Methods	20
3.1	Beta Model	20
3.1.1	Interpretation of the Beta Model	21
3.1.2	Training the Beta Model	23
3.2	Normalizing Flow Models	24
3.2.1	Spline Coupling Normalizing Flows	24
3.2.2	General Normalizing Flow Model	24
3.2.3	KL-Divergence and Direct Optimization	25
3.2.4	ELBO and SVI	26
4	Experimental Setup	27
4.1	Validation of Incorrectness in Benchmark Datasets	27
4.2	Noise Filtering Experiment	27
4.3	Tree Embedding Experiment	27

5	Results	27
6	Discussion	27

GNN Interpretability Using Bayesian Inference

Shalin Patel^{1,2}

¹*Division of Applied Mathematics, Brown University*

²*Department of Computer Science, Brown University*

April 15, 2023

Abstract

1 Introduction

Graphs serve as a natural repository for information in many real-world applications ranging from social, informational, chemical, and biological domains [1]. Especially as data becomes more and more unstructured, graphs represent a flexible manner for storing and relating different nodes and their related features [2]. Indeed, graphs represent one of the most general mathematical structures for relating data and are seeing increasing use in modeling phenomenon such as social networks and gene regulatory networks [2, 3]. For the purposes of this work, given a set of vertices V , node features $\mathcal{X} : V \rightarrow \mathbb{R}^d$, a set of edges $E \subseteq V \times V$, and weights on the edges $W : E \rightarrow [0, 1]$, we consider the graph $G = \{V, \mathcal{X}, E, W\}$. Additionally, we let the space of all graphs for a given set of vertices V be \mathcal{G} . Below in figure 1, a simple visualization of this definition can be seen for a cyclic graph of order 3.

1.1 Graph Neural Networks

To deal with the proliferation of graphs in computing and the need to construct models that consider graphs as a first-class member of the modeling process, a class of models known as

Graph Neural Networks have emerged (GNN) with state of the art performance on a variety of classification and regression tasks [4]. Specifically, GNNs and their early iterations in GCNs took inspiration from CNNs that represented applying successive convolution operations on regular grids of information, such as images, to compose local features in the grid in to higher-level predictions [5]. At a high level, most GNN frameworks can be split into three steps **MSG**, **AGG**, and **UPD** representing a messaging step, aggregation step, and update step, respectively.

At a layer l in a GNN model ϕ , the update of the hidden state of the model occurs first by sending messages for all $(v_i, v_j) \in E$ as a function of the hidden state \mathcal{H}_i^{l-1} and \mathcal{H}_j^{l-1} as well as the weight $W_{ij} := W(v_i, v_j)$. Specifically, we have

$$m_{ij}^l := \text{MSG}(\mathcal{H}_i^{l-1}, \mathcal{H}_j^{l-1}, W_{ij})$$

Then, a GNN performs an aggregation step wherein it calculates an aggregate message for every vertex $v \in V$. Let $\mathcal{N}_k : V \times E \rightarrow \mathcal{P}(E)$ be a function that returns the edges in the k -hop neighborhood of a node. Then, we can formally write the aggregation step as

$$M_i^l := \text{AGG}(\{m_{ij}^l \mid v_j \in \mathcal{N}_k(v_i)\})$$

Then, finally, at each node, the GNN takes a nonlinear function (often a neural network of some sort) and applies it to this aggregated message M_i^l along with the hidden state \mathcal{H}_i^{l-1} to get the new hidden state.

$$\mathcal{H}_i^l := \text{UPD}(\mathcal{H}_i^{l-1}, M_i^l)$$

When composed in layers, this forms a full Graph Neural Network. Note that in this framework, $\mathcal{H}_i^0 := \mathcal{X}_i$. Based on the task type, either node or graph classification in this work, further layers may be added on top of the final output. For example, in graph

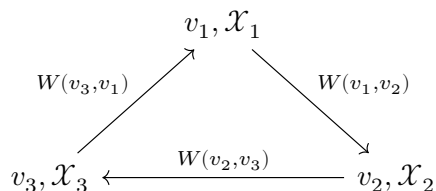


Figure 1: An example graph as related to the terminology laid out above

classification, it is often the case that the final node embeddings are concatenated and then run through an MLP to get a final classification for the whole graph [4].

The specific layers used in this work are Graph Convolution Layers also known as GCNs [6]. In the context of the framework above, the **MSG** sends weighted and normalized node features from the $l - 1$ st layer where the normalization is by the out-degree of the sending node and the weight of the message coming from \mathcal{W}_{ij} . In the **AGG** step, all of these messages are summed together. Finally, the **UPD** step applies a neural network, usually a trainable linear layer combined with a non-linear activation function to provide a non-linear update step.

1.2 Interpretation on GNNs

Given a GNN, it is natural in many fields such as computational biology to perform interpretation on the model in order to gain further insights. For example, in the case of RNA-seq data, a natural question is to determine important regulatory pathways between genes that could be related to eventual up or down regulation of a target gene [3]. One natural way to perform this task is to train a GNN on the RNA-seq data for a node-classification task and feed it a large graph G with many redundant edges. Given a GNN model ϕ with l layers and a target gene $v_i \in V$, we would like to determine $\mathcal{E}_i \subseteq \mathcal{N}_l(v_i, E)$ as well as $\mathcal{W}_i : \mathcal{E}_i \rightarrow [0, 1]$ such that $\mathcal{E}_i, \mathcal{W}_i$ represent the most important subgraph for the model ϕ to perform its predictions for the input vertex v_i . While there are a few criteria for determining importance, we consider importance to be the maximal mutual information between the original model with its inputs and the same model with the estimated subgraph $\mathcal{E}_i, \mathcal{W}_i$. Written more formally, we wish to discover

$$\arg \max_{\mathcal{E}_i, \mathcal{W}_i} \text{MI}(\phi(v_i, \mathcal{X}, E, W), \phi(v_i, \mathcal{X}, \mathcal{E}_i, \mathcal{W}_i))$$

This is a computationally hard problem as a brute force search would take $O(2^{|E|})$ time even when discounting the weight array \mathcal{W}_i . In practice, discovering \mathcal{E}_i is ignored and most of the importance discovery is done through learning a suitable \mathcal{W}_i while letting $\mathcal{E}_i = E$.

However, because of the given task, and the various properties we would like to see in a reasonable interpretation of a GNN model, there are many routes that have been taken to interpret these models. As will be shown in §2, there have been a few non-bayesian attempts to solve this problem. The goal of this work is to analyze these methods

and then suggest a new Bayesian method to solving the issue of searching for the best subgraph for a trained GNN to perform post-hoc analysis of importance. Furthermore, an added benefit of utilizing a Bayesian approach is that a full conditional distribution over the importance graph is learned giving researchers an even larger level of insight into their model that goes beyond just a simple edge mask.

1.3 Bayesian Inference

Recently, in deep learning literature there has been a rise in utilizing Bayesian methods to create Bayesian Neural Networks in order to provide uncertainty aware predictions [7]. While primarily concerned with giving estimates for failure modes and reducing overfitting within deep learning methods, the synthesis of Bayesian methods and deep learning models has imbued them with a greater sense of interpretability and introspectability. In the context of GNN interpretation, modeling the subgraph $\mathcal{E}_i, \mathcal{W}_i$ as a joint distribution allows for conditioning on certain edge weights and imbues the interpretations that are derived with a greater sense of introspectability. Figure 2 gives a good overview of the deep learning analogues for point estimate neural networks. In the same way, analogues will be utilized in the interpretation task in order to get the same benefits that have already been outlined in BNNs. In the Bayesian paradigm, a distribution \mathcal{P} is treated as the belief in the occurrence of a given event from the distribution rather than the limit of the frequencies of each event as in the frequentist scheme. Furthermore, prior beliefs are thought to inform posterior beliefs. In the context of interpretability this is important as the belief for a given interpretation is dependent on the domain that it is brought up in. For example, in social networks one may expect relatively dense explanations while in biology they would tend to be sparse [1] [3]. Generally speaking, given a hypothesis H representing the prior belief for the state of a system and some data D , the posterior probability $\mathcal{P}(H \mid D)$ can be calculated as

$$\mathcal{P}(H \mid D) = \frac{\mathcal{P}(D \mid H)\mathcal{P}(H)}{\mathcal{P}(D)}$$

and in this way, the posterior is conditioned by both the prior belief and the evidence that the data presents. While there are a variety of different techniques that can be used to update the prior belief into a posterior distribution as seen in figure 2, in this paper only stochastic variational inference (SVI) and Bayes-by-backprop are utilized.

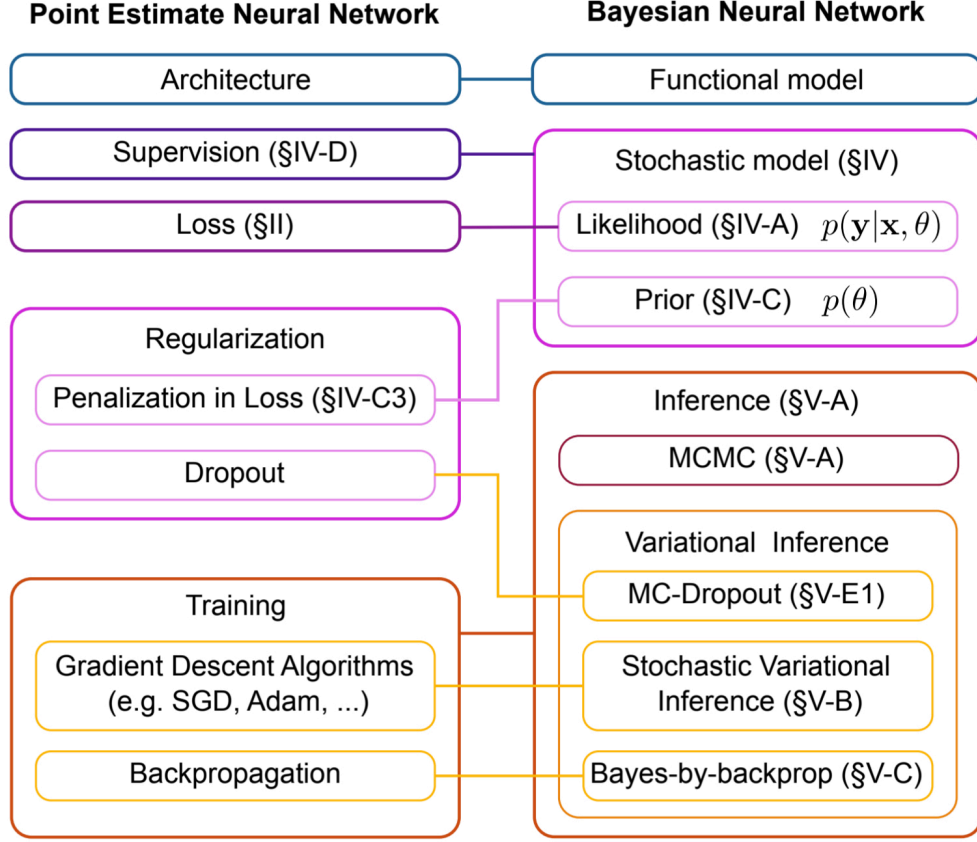


Figure 2: An overview of the corresponding structures in a standard neural network and a bayesian neural network. Originally appeared in [7].

1.3.1 Stochastic Variational Inference (SVI)

While other inference methods such as MCMC (with popular algorithms including HMC and NUTS [8] [9]), allow exact sampling from the posterior distribution, these methods have proven unpopular with the BNN community due to their algorithmic complexity and lack of scalability to larger models. Hence many communities use SVI which is not an exact method. In SVI, there is a family of distributions $q_\phi(H)$ which are parametrized by parameters ϕ . A common example would be the family of normal distributions parametrized by their mean and covariance structure. The goal of SVI is to approximate the posterior $\mathcal{P}(H | D)$ as closely as possible by $q_\phi(H)$. The most common measure of approximation in

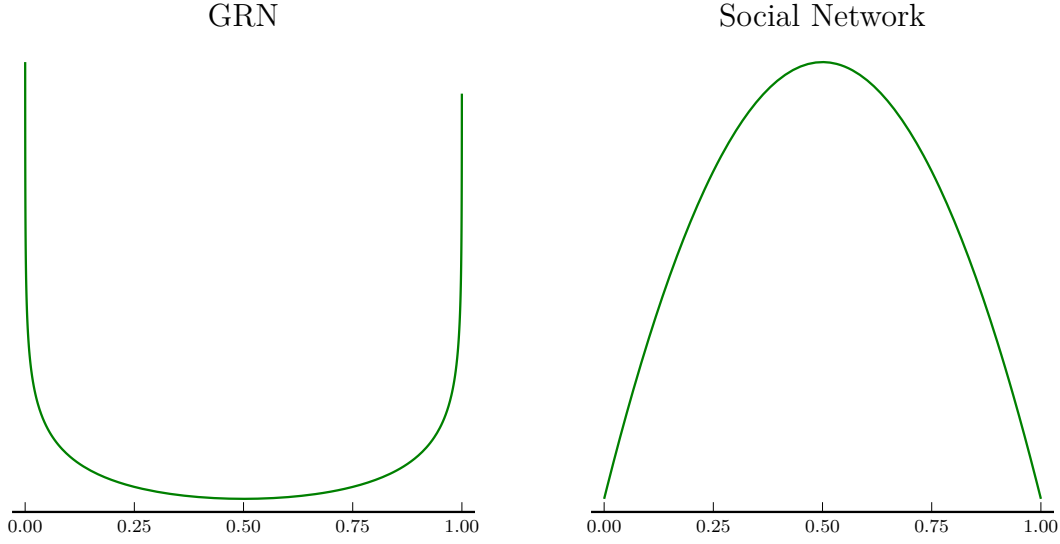


Figure 3: Idealized prior distributions for GRNs and Social Networks based on the Beta distribution. The displayed distributions are $B(0.95, 0.95)$ and $B(2, 2)$ respectively

probability space is given by the Kullback-Leibler divergence (KL-divergence). While not a proper metric over the space of distributions, it does give a computationally-reasonable method to optimize against ϕ to get as close a match as possible. Specifically, SVI aims to minimize

$$D_{KL}(q_\phi \parallel \mathcal{P}) = \int_H q_\phi(H') \log \frac{q_\phi(H')}{\mathcal{P}(H' \mid D)} dH'$$

This is still problematic since the quantity $\mathcal{P}(H \mid D)$ would still need to be calculated. Hence, it is sufficient to optimize against the ELBO which serves as a lower-bound for the KL-divergence. The ELBO is defined as

$$\log \mathcal{P}(D) - D_{KL}(q_\phi \parallel \mathcal{P}) = \int_H q_\phi(H') \log \frac{\mathcal{P}(H', D)}{q_\phi(H')} dH'$$

Note here that $\log \mathcal{P}(D)$ is just a constant meaning that minimizing the KL-divergence is the same as maximizing the ELBO. Note that, generally speaking, the families q_ϕ tend to come from the exponential family of distributions and the parameters for these families are then just optimized using a typical SGD algorithm such as ADAM [10].

1.3.2 Bayes-by-backprop

While SVI provides a good framework for Bayesian inference, it does not quite work for deep learning applications because stochasticity stops backpropagation from going through a neural network. To mitigate this problem, the usual reparametrization technique used in creating variational autoencoders (VAEs) [11] is combined with SVI to create a deep-learning friendly SVI algorithm. In this variation, a simple non-parametrized random variable $\epsilon \sim q(\epsilon)$ is sampled. To obtain the family $q_\phi(\theta)$, a deterministic transformation $t(\epsilon, \phi)$ is applied such that $\theta = t(\epsilon, \phi)$ has the property that $\theta \sim q_\phi(\theta)$. To obtain such a t , only a certain class of functions can be utilized. These functions are broadly known as bijectors and require t to be a diffeomorphism. In more detail, let $t : M \rightarrow N$ be a differentiable map, then t is a diffeomorphism if it is a bijection and its inverse $t^{-1} : N \rightarrow M$ is differentiable as well.

Generally speaking, the exponential family of distributions can all be constructed from such transformations meaning that they are good candidates for Bayes-by-backprop. Note though, that because of the transformation t , the formula for the ELBO changes to the following

$$\int_{\epsilon} q_{\phi}(t(\epsilon, \phi)) \log \frac{\mathcal{P}(t(\epsilon, \phi), D)}{q_{\phi}(t(\epsilon, \phi))} |\det(\nabla_{\epsilon} t(\epsilon, \phi))| d\epsilon$$

This is much friendlier to compute since ϵ is now a constant with respect to ϕ and lets us perform SVI through multiple layers of transformations simply by using bijectors like t .

1.4 Normalizing Flows

The technique that was described in §1.3.2 is more generally known as a normalizing flow. While it was described earlier in the context of a reparametrization technique in which the t are fixed, there is no such restriction in reality. More concretely, the t do not have to be simple functions but, rather, can be learnable functions in their own right. This allows one to use the normalizing flow technique to perform tasks like density estimation and distribution fitting with a very flexible class of transforms that take a simple distribution like a standard multivariate normal and make them into any computable distribution [12]. Let the transformations of the base distribution be defined as $g = g_n \circ g_{n-1} \circ \dots \circ g_1$ with inverse $f = g_1^{-1} \circ g_2^{-1} \circ \dots \circ g_n^{-1}$. Then we know that the determinant of the Jacobian of f is given by the product of the determinants of the Jacobians at each intermediate evaluation

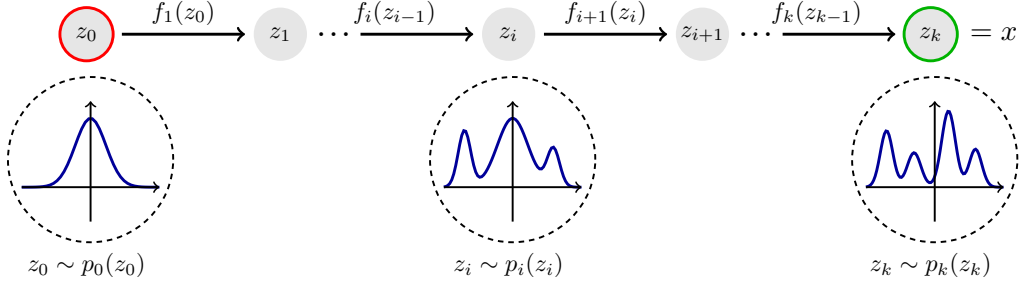


Figure 4: Chaining learnable bijectors to transform a base distribution to a more complicated distribution from [13]

of the flow. This allows for more and more complicated transformations by introducing more and more learnable layers as can be seen in figure 4. This structure is very similar to that of an artificial feed-forward neural network. As an example, the simplest form of a normalizing flow is

$$g_i(x) = Ax + b$$

with the learnable parameters here being the matrix A and bias vector b . As long as A is an invertible matrix, we have a bijective function that can be used as a normalizing flow layer. Note that these linear layers can be interleaved with activation functions to provide non-linear transformations. This is important as a linear transformation of an exponential family will remain exponential so an element of non-linearity is required (as is the case with MLPs). While RELU is not invertible, a formulation like leaky-RELU can be used for this task [14]. Still these are not super expressive. For a normalizing flow with universality, this paper utilizes rational quadratic spline based flows [15]. When combined with variational inference over the prior base-distribution, this allows for a very flexible estimation of the posterior distribution no matter how complex.

2 Related Work

When it comes to GNN interpretability, there are a few main methods. The first that started the field of GNN interpretability was GNN Explainer [4] which also provided a suite of general benchmarks that most methods have utilized as a framework for analyzing the effectiveness of their explainer framework. Another major piece of work in the field has been the parametrized-graph explainer (PGExplainer) [16] that took GNNExplainer and parametrized it with a deep neural network for faster inference times and more robust interpretation. Along with these two, a few other more recent explainers such as SubgraphX [17] and Gem [18] have introduced new ideas into the field with a variety of approaches to the problem of GNN interpretability. To date, there seems to be no fully Bayesian method to the problem of GNN interpretability.

In addition to these works, the work of SERGIO [19] will be introduced as it will be utilized later on to generate a new class of experiments that GNN Interpretability methods can be benchmarked against. This work provides causal graph structures that give a guaranteed groundtruth for interpretation.

2.1 GNN Explainer

The full version of GNNExplainer attempts to learn both a node interpretation and edge interpretation. For this work, only the edge interpretation part of the framework was utilized. GNN Explainer attempts to solve the objective outlined in §1.2, by only trying to learn \mathcal{W}_i while treating $\mathcal{E}_i = E$. In this framework, GNN Explainer enforces that for any $e \in E$, $W(e) \geq \mathcal{W}_i(e)$. Then to get the argmax, GNNExplainer treats \mathcal{W}_i as a random variable. Then the goal get transformed to

$$\arg \min_{\mathcal{W}_i} \mathbb{E}_{w \sim \mathcal{W}_i} [H(\phi(v_i, \mathcal{X}, E, w))]$$

This still remains intractable, so GNNExplainer attempts to make this simpler by using Jensen’s inequality. Note that this is not a reasonable application of Jensen’s since ϕ as a GNN has almost no hope of being convex. Nonetheless, using Jensen’s inequality gives

$$\arg \min_{\mathcal{W}_i} H(\phi(v_i, \mathcal{X}, E, \mathbb{E}[\mathcal{W}_i]))$$

This is still quite intractable if \mathcal{W}_i is a full joint distribution over all $e \in E$. Therefore, GNNExplainer attempts to use a mean field approximation for \mathcal{W}_i where the edge interpretation is decomposed into the product of Bernoulli distributions meaning that each edge weight is an independent Bernoulli distribution with mean equal to the underlying probability of the variable. Specifically,

$$\mathcal{P}(\mathcal{W}_i) = \prod_{(v_j, v_k) \in E} \mathcal{W}_i[v_j, v_k]$$

with each $\mathcal{W}_i[v_j, v_k]$ is a value between $[0, 1]$ representing a Bernoulli variable for each edge in the underlying graph as defined by E . In this case, if the classification for a node is c , GNNExplainer performs direct gradient descent on this array of values to minimize

$$\arg \min_{\mathcal{W}_i = \{\mathcal{W}_i[v_j, v_k] | (v_j, v_k) \in E\}} - \sum_{c=1}^C \mathbb{1}_{y=c} \log \mathcal{P}(\phi(v_i, \mathcal{X}, E, \mathcal{W}_i) = c)$$

While there is some probabilistic formulation here, in effect, GNNExplainer optimizes an adjacency matrix in $[0, 1]$ against the mutual information of the model given the edge weights and the model with the original graph. This means that GNNExplainer learns no conditional structure between edges and does not take the graph dynamics into account while training. This is further emphasized with the fact that a mean-field approximation was used to assume conditional independence between the edges of the underlying graph. Hence, it is an algorithm that provides only a summary of the interpretation using assumptions that are not generally applicable to GNNs.

2.1.1 Benchmark Datasets

As one of the first explainer methods for GNNs, GNNExplainer created a set of synthetic datasets that serve as the canonical datasets for GNN Interpretability. The goal of this section is to describe these datasets and the perceived shortcomings in these datasets that led to an exploration of their validity and a setup for the experiments produced later that demonstrate the incorrectness of these datasets for the stated task.

The main dataset focused on in this paper is the Tree-Cycles dataset [4]. In this dataset trees of depth three are attached to cycles of length six in order to form and aggregate dataset. A GNN node classification task entails predicting whether a given node is either in a tree portion of the graph or in the cyclic portion of the graph with no given node features.

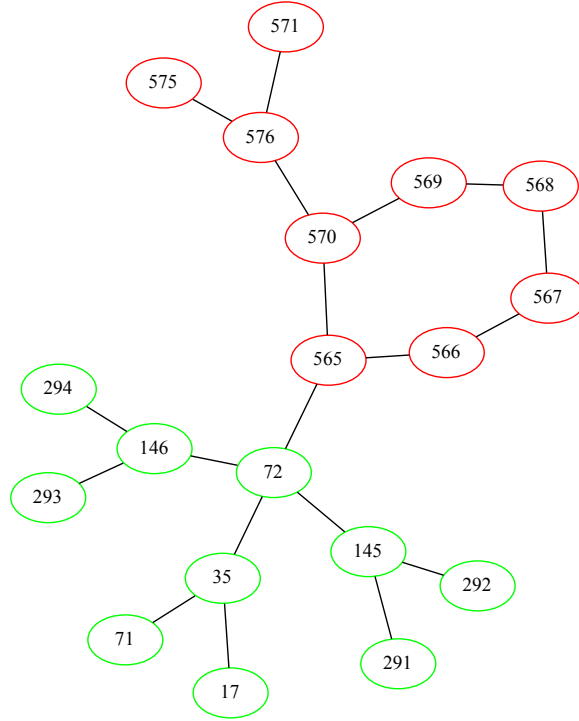


Figure 5: A look at the tree-cycles dataset at a three-hop neighborhood around node 565. In green are nodes classified as tree nodes and in red are nodes classified as cycle nodes. The dataset is almost 50% balanced between these two types.

The idea here is that the GNN can only rely upon the structure of the graph for its node classification and all its information must come from the edges. Hence interpretation on the edges of the GNN would reveal only information that could be gleaned from the graph structure. In figure 5, one can see an example of a portion of the dataset looking at a three-hop neighborhood around node 565.

While this is a great construction to test an interpretation method, given that the GNN only relies on the graph structure for prediction, it is difficult to imagine what the ground truth for a given dataset is. The paper that introduced GNNExplainer proposed that the groundtruths be motifs in the graph. So if a node was in a cycle portion, the groundtruth would be the edges in the cycle and if a node was in the tree portion, the groundtruth

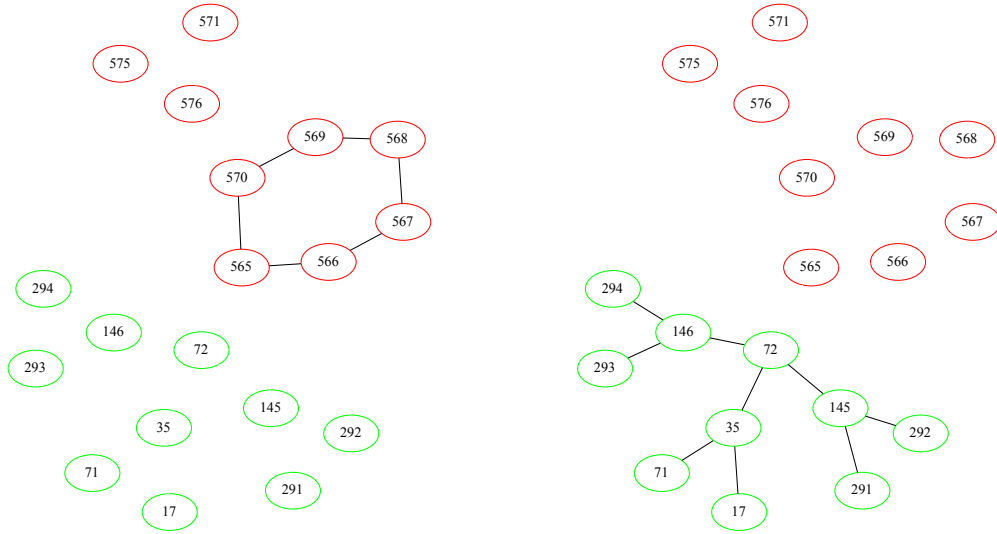


Figure 6: Demonstrations of the proposed groundtruths under [4] for the tree-cycles dataset. On the left is the proposed groundtruth for a node in the cycle (565) and on the right is the proposed ground truth for a node in a tree (72).

would be the edges of the tree. This can be seen in figure 6 which shows the proposed ground truths. While this is a valid task for an interpretation technique to attempt to solve, it does not have direct bearing on the task that the GNN was trained on and it does not have direct bearing on the mutual information framework that forms the theoretical underpinning for GNN interpretability.

In a simple example, suppose a GNN is trained on the tree-cycles dataset. While it might be nice if the GNN needed all the edges in a cycle structure to determine that the node is, indeed, in the cycle, the GNN could have just as easily learned to use five edges from the cycle to make its predictions. Even if a theoretical GNN interpretation model was perfect, the fact that the GNN itself does not use the sixth edge means that an interpretation technique is doomed to max its accuracy score at $5/6$ which would make it impossible to compare between methods. Furthermore, a GNN may learn to mix motifs when making its prediction. Consider node 565 in the example from figure 5. While this node is in the cycle portion of the graph, the GNN could very easily learn that the

node is *adjacent* to the tree structure detected in node 72 and learn to make the inverse decision in this case. Notably, there is no guarantee that a GNN learns the motifs as the important substructures and there is little chance that across nodes, it consistently learns these rules. Indeed, it will be shown later that GNNExplainer itself struggles to meet its $> 90\%$ accuracy scores for this benchmark in replication studies [17] [18] and that a thorough search through all connected subgraphs fails to yield this structure as the ground truth.

While GNNExplainer suggests a few other benchmark datasets, they all suffer from the same issue. Namely, they claim that the groundtruth is the embedded motif structure, but a simple tests reveal that this is not consistently true and nor should it be true in the general case. Hence, a goal of this paper is to also provide a set of alternative benchmarks against which to evaluate GNN interpretability.

2.2 Parametrized-Graph Explainer

Parametrized-Graph Explainer (PGExplainer for short) aims to take the GNNExplainer process and parametrized so that after training a deep neural network, new explanations per node could be generated with the much smaller cost of conducting inference on a given node v_i .

In the PGExplainer model, they attempt to construct a generative probabilistic model for the underlying subgraph by assuming that the explanatory graph is a Gilbert random graph [20] where the edges are conditionally independent of each other, much like GNNExplainer. Hence, the probability of a random subgraph being chosen is given in the same exact way as GNNExplainer. For clarity, this is

$$\mathcal{P}(\mathcal{W}_i) = \prod_{(v_j, v_k) \in E} \mathcal{W}_i[v_j, v_k]$$

and the learning objective, which starts the same as GNNExplainer, becomes the following as they avoid using Jensen's or the mean field approximation

$$\arg \min_{\mathcal{W}_i = q_\Theta} \mathbb{E}_{\mathcal{W}_i \sim \mathcal{W}_i} [H(\mathcal{P}(\phi(v_i, \mathcal{X}, E, \mathcal{W}_i)))]$$

Note here that the distribution \mathcal{W}_i is to be generated by a DNN that is specified by q and takes as input the parameters Θ . To sample these graphs in a manner that allows for

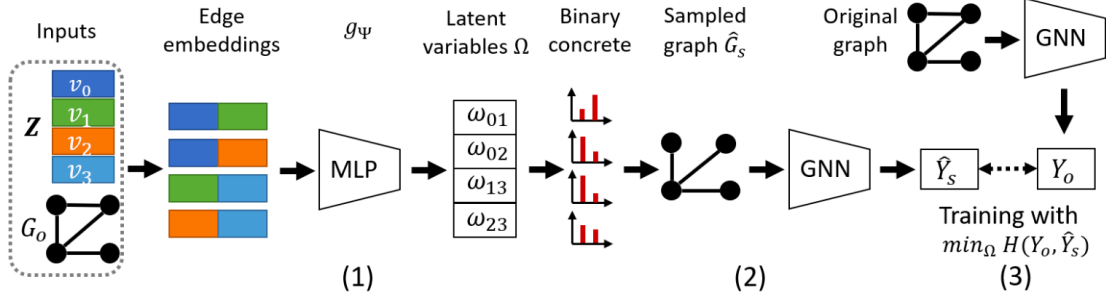


Figure 7: A convenient overview of the PGExplainer pipeline (with slightly different variable names and setting etc.) [16]

training over the global view of the node classification task, the PGExplainer framework does the following.

1. Most node classification GNNs have a bunch of GNN layers before a final MLP that takes the graph embeddings obtained from the GNN layers and performs a final prediction on the nodes classification. The PGExplainer framework denotes this graph embedding step as ϕ_0 and extracts it from the GNN task. Let

$$Z = \phi_0(v_i, \mathcal{X}, E, W_i)$$

be the graph embedding calculated with a sampled subgraph W_i .

2. To calculate the distribution $\mathcal{W}_i(v_j, v_k)$, the PGExplainer lets g be a MLP network with shared parameters Θ . As an input, this MLP takes the concatenated values of the graph embedding Z for node i and the nodes j and k as they represent the edge (v_j, v_k) . Hence, we have

$$\mathcal{W}_i(v_j, v_k) = g_{\Theta}([Z_i; Z_j; Z_k]) \quad \forall (v_j, v_k) \in E$$

Note here that all edge distributions are independent with respect to i, j, k .

3. Finally, given this distribution. The parameters Θ are trained by sampling K subgraphs using the independent edge distributions (utilizing a reparametrization technique) and then optimizing the above objective with these samples. Let $W_i^{(k)}$ represent

the k th sampled subgraph. Then the following objective function represented the final target against which PGExplainer was optimized

$$\arg \min_{\Theta} - \sum_{v_i \in V} \sum_{k=1}^K \sum_{c=1}^C \mathcal{P}(\phi(v_i, \mathcal{X}, E, W)) \log \mathcal{P}(\phi(v_i, \mathcal{X}, E, W_i^{(k)}))$$

Together this gives the PGExplainer framework. A convenient outline from their paper can be seen in figure 7. Note that this framework was tested against the same benchmarks that were given by GNNExplainer. While this gives a more probabilistic framework, it suffers, again, from learning a conditionally independent distribution per edge which disallows further introspection and also ignores the conditional structure while generating subgraphs. This method is better in that it trains these distributions globally across nodes which means that more structure is being captured on the average and allows the model to be universal for a dataset. In effect, the combined training allows for a blurring of the edge importances across different nodes which makes it more useful and generalizable when looking at the edge importance of a specific node.

2.3 Other Explainer Frameworks

While there have been a few other explanation frameworks that have emerged in the time following GNNExplainer [4] and PGExplainer [16], most featured roughly similar performance or design. There are, though a couple frameworks that provide an interesting comparison to the two just mentioned.

2.3.1 SubgraphX

This method is different than most methods in that it does not attempt to learn a \mathcal{W}_i . Instead, it actively searches for a \mathcal{E}_i and lets $\mathcal{W}_i(v_j, v_k) = 1 \ \forall (v_j, v_k) \in \mathcal{E}_i$. It does this via a Monte-Carlo Tree Search algorithm that is informed by computing Shapley values for proposed subgraph structures and combining them in the tree search [17]. Additionally, this paper eschews the traditional accuracy/AUC evaluation metric used by GNNExplainer and PGExplainer in favor of a Fidelity/Sparsity framework. Crucially, they note that the task being defined by these interpretation models is not detection of human-interpretable groundtruth motifs, but rather, fidelity to the original predictions made by the full GNN model.

2.3.2 GEM

The GEM framework attempts to use Granger Causality to guide its exploration process in learning the \mathcal{W}_i function. The most interesting contribution of this paper to this study was the recognition that the groundtruths determined in the GNNExplainer and PGExplainer works were a bit arbitrary. Certainly, in real-life datasets the motifs that drive a GNN performance are not always apparent and need to be discovered rather than rediscovered. Hence, these benchmarks are a little suspect as they have little bearing on the process of using a GNN interpretation method on a real-world problem.

2.4 SERGIO

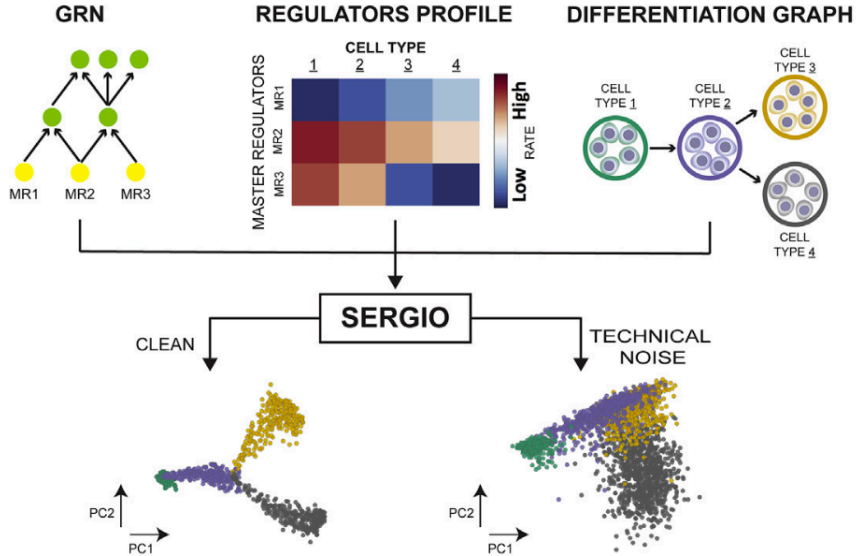


Figure 8: A graphic from the SERGIO paper detailing the inputs and outputs to the SERGIO process [19]. Specifically, a ground truth GRN is utilized to generate the data and recovering this GRN from the data could be a task for a GNN interpretation task.

SERGIO is a model for simulating single cell gene expression data with guidance from gene regulatory networks [19]. Before SERGIO, most methods of simulating single cell expression data came from analyzing the statistical properties of real-life single cell datasets and then matching these properties with appropriate distributions that could then be

sampled from in order to generate new data. While these methods got more and more sophisticated in the number of statistics they matched against, there was no inclusion of gene regulatory networks (GRNs) which are crucial for single cell expression profiles both in the steady state and dynamical regimes. While these methods got more and more sophisticated in the number of statistics they matched against, there was no inclusion of gene regulatory networks (GRNs) which are crucial for single cell expression profiles both in the steady state and dynamical regimes.

SERGIO aimed to bridge this gap and created a method that both matched the statistical distributions of experimental expression profiles while utilizing GRNs as the core of the modeling process as seen in figure 8. Crucially, though, the GRN underlying the final expression profile is entirely causal in driving the profiles that it generates and SERGIO maintains the ability to add technical noise into the proposed expression profile. This makes it a perfect setup for an experiment in GNN interpretability where the goal of an interpretation method would be to recover the underlying GRN from a GNN trained on predicting cell type from the expression data. While biological in origin, the abstract problem is perfect for a GNN interpretation task to be benchmarked against.

3 Methods

In this paper, three different probabilistic formulations exist for the underlying edge importance model. All three of these models rely upon the excellent `Pyro` [21] framework for implementation and inference. Additionally, all GNN models are trained through the `pytorch_geometric` [22] and `pytorch` [23] frameworks.

3.1 Beta Model

The first method used in this paper is a prior in which all Beta distributions are considered independent of each other. Specifically, we assume that $\mathcal{E}_i = E$ and that

$$\mathcal{W}_i = \{\mathcal{W}_i(v_j, v_k) \mid (v, j, v_k) \in E\}$$

with

$$\mathcal{W}_i(v_j, v_k) = \mathbb{E}[Beta(\alpha_j, \beta_k)]$$

with $Beta(\alpha_{j,k}, \beta_{j,k})$ representing the prior Beta distribution on edge (v_j, v_k) with specific parameters $\alpha_{j,k}$ and $\beta_{j,k}$. Note, we define the Beta distribution as

$$\mathcal{P}(Beta(\alpha, \beta) = x) = \frac{x^{\alpha-1}(1-x)^{\beta-1}}{B(\alpha, \beta)}$$

$$B(\alpha, \beta) = \frac{\Gamma(\alpha)\Gamma(\beta)}{\Gamma(\alpha + \beta)}$$

where Γ is the canonical Gamma function [24]. Given this, the goal of the interpretation task is to learn a variational family $q_\phi(H)$ that most closely resembles the posterior distribution when the categorical distribution

$$\phi(v_i, \mathcal{X}, E, \mathcal{W}_i)$$

is conditioned on the full model

$$\phi(v_i, \mathcal{X}, E, \mathcal{W})$$

where $\mathcal{W}(e) = 1$ for all $e \in E$. For the sake of this experiment, the posterior distribution is also assumed to be a set of Beta distributions but fully conditional on each other. The goal, then is to learn posterior values $\hat{\alpha}_{j,k}$ and $\hat{\beta}_{j,k}$. Given these values, the final explanation is

$$\mathcal{W}_i(v_j, v_k) = \mathbb{E}[Beta(\hat{\alpha}_j, \hat{\beta}_k)]$$

which has an easily derived closed form.

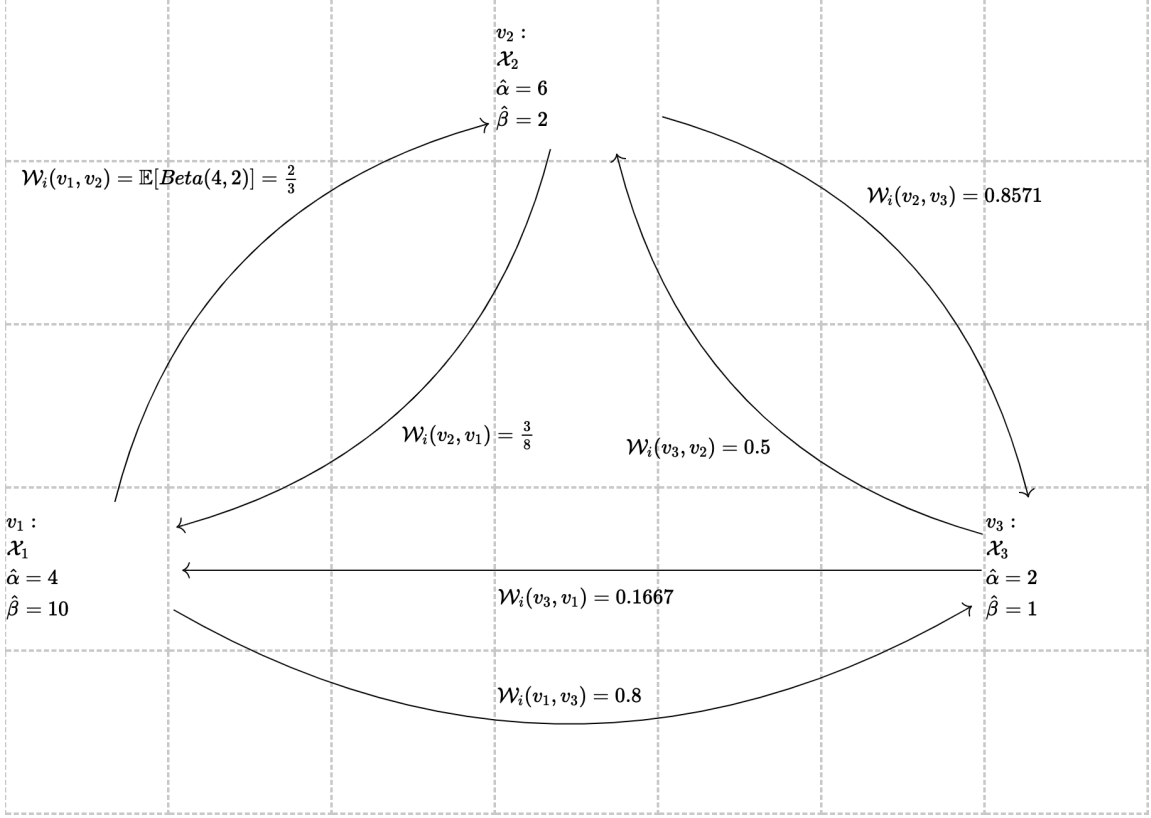


Figure 9: An example of a Beta posterior that shows information flowing from v_1 to v_3 .

3.1.1 Interpretation of the Beta Model

There is a wide array of literature on the use of Exponential-families for the modeling of edge weight priors. In particular, the work of Bolla [25] is important. In this work, edge weights are modeled by conditionally independent Beta distributions. The parameters of these Beta distributions are updated via a closed-form solution but it serves as a good model for prediction propagation of information or material from one node to another and converging on a steady-state for the propagation. In the case of GNNs, one can imagine the MSG operation as the sending of information. The dense layers in the Upd step, then, learn the weight to assign to each incoming and outgoing message. In this vein, the Beta model can approximate this "attention" that is paid in the Upd step. Hence, the goal of this model is to serve as an approximation of this process and encode the steady-state flow

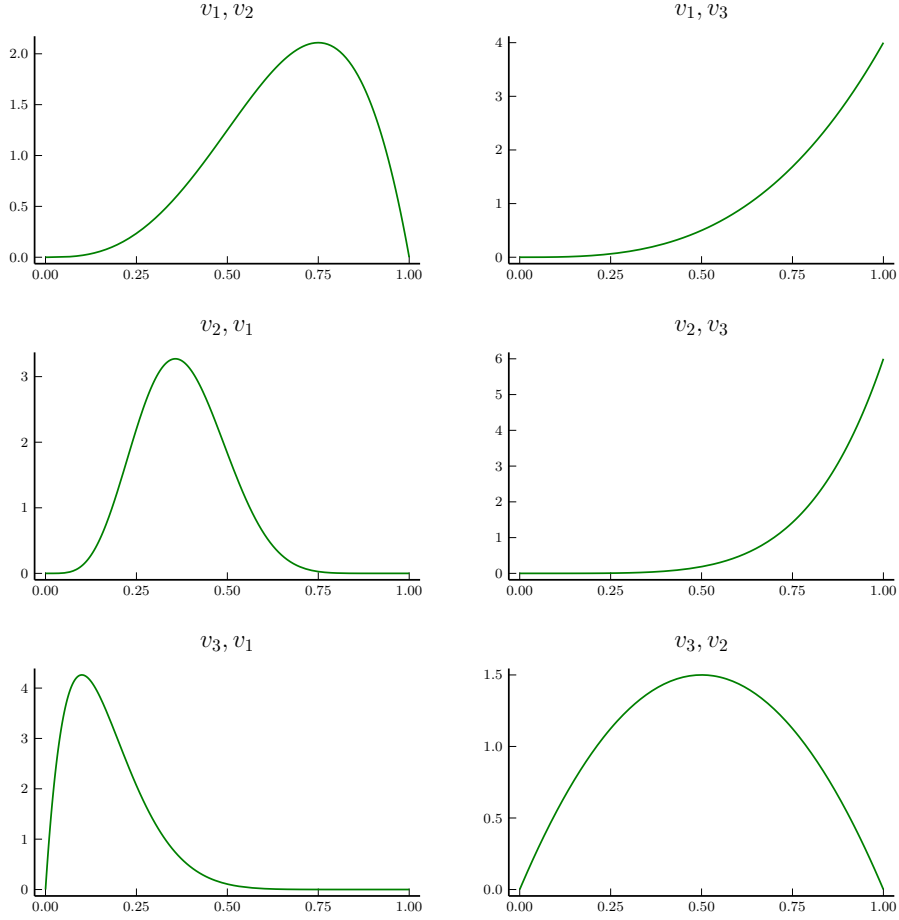


Figure 10: Posterior distributions for each edge in 9

of information in the model.

In this model, the α values serve to describe the affinity for information to flow out of a node while the β values tend to describe the affinity for information to flow into the node. Together, they describe the steady state flow of information and perfectly describe many networks in which pathways of information lead to end-goal expression. Indeed, since GNNs tend to embed this type of information flow in a deep-learning setting, it serves to reason that such a prior would be a good encapsulation of the process of information flow, especially at steady state. A typical example of this is gene expression in biology [3] where paths of edges represent regulatory pathways directly.

An example of this flow can be seen in figure 9. In this figure, we consider a hypothetical posterior for this model and demonstrate how it describes the flow of information from node v_1 to v_3 via these α and β parameters. Additionally, in figure 10, one can see the posterior distribution of each edge. Notably, there is no conditional independence in this model as changing the parameter on one node changes all adjoining edges.

3.1.2 Training the Beta Model

While [25] demonstrated a novel technique to train the parameters to get the true posterior in the limit, this paper will use a standard SVI setup to train the posterior. In the `Pyro` framework, all SVI runs need two things: the forward model and the variational guide. In listing 1, both the model is shown and the guide follows a very similar setup since it has the same exact structure. Note that in both cases the mask is sampled from a beta distribution as defined above. Most GNNs have an effective computational graph size as denoted by the number of layers that are in the model. This effective computational graph is generally, the l -hop neighborhood around v_i so we only consider interpretation on $\mathcal{N}_l(v_i, E)$ as the other nodes cannot have any influence. Analogously, let all the nodes in this l -hop neighborhood be $V_{i,l}$.

Algorithm 1 The model setup for the Beta model

Require: $v_i \in V, \bar{\alpha} > 0, \bar{\beta} > 0$

Require: $c \sim \phi(v_i, \mathcal{X}, \mathcal{N}_l(v_i, E), \mathcal{W})$

$\alpha \leftarrow [\bar{\alpha} \mid \forall v_j \in V_{i,l}]$

$\beta \leftarrow [\bar{\beta} \mid \forall v_j \in V_{i,l}]$

$W_i(v_j, v_k) \sim \text{Beta}(\alpha_j, \beta_k) \quad \forall (v_j, v_k) \in \mathcal{N}_l(v_i, E)$

$\hat{y} \leftarrow \phi(v_i, \mathcal{X}, \mathcal{N}_l(v_i, E), W_i)$

$\hat{c} \sim \hat{y}$

The SVI algorithm then optimizes against the α and β parameters to match the variational distribution \hat{y} as closely as possible to the full distribution $\phi(v_i, \mathcal{X}, \mathcal{N}_k(v_i, E), \mathcal{W})$. Note that in the case of a graph classification task, the model ϕ simply loses its dependence on v_i and we compare against $\phi(\mathcal{X}, E, \mathcal{W})$. They are the exact same formulation. In each epoch of the SVI inference, only one sample is used to get an estimate of the ELBO as is the standard practice [7]. While this gives a noisy estimate, over time, the value of the

ELBO should increase to indicate a better model fit.

3.2 Normalizing Flow Models

In this work, there are two specific normalizing flow models that are tested. In one, the system is trained using SVI to utilize the ELBO as the objective, while in the other a simple KL-divergence is computed and the parameters of the normalizing flow are directly optimized using an appropriate SGD algorithm.

3.2.1 Spline Coupling Normalizing Flows

As mentioned in section §1.4, for a fully universal normalizing flow model, more expressive transformations are required than invertible affine transformations. One such method comes from spline coupling normalizing flow layers as described in [26]. In this work, spline transforms are combined with coupling layer transforms.

First, we describe coupling layer transforms. In this category of transforms, the output of a layer consists of two parts. Let $z \in \mathbb{R}^D$ be the data to be transformed. Then we split this data such that $z_1 \in \mathbb{R}^d$ and $z_2 \in \mathbb{R}^{D-d}$. They are then transformed according to

$$\begin{aligned} x_1 &= z_1 \\ x_2 &= g_{\theta(x_1)}(z_2) \end{aligned}$$

with the final output being $x = [x_1; x_2]$. Plenty of different $g_{\theta(x_1)}$ have been proposed. In this work, the neural linear splines from [26] are used due to their competitive performance compared to quadratic or cubic splines as well as increased computational performance.

Most importantly, these coupling flows are able to capture full conditional distributions and have been used in models such as VAEs and generative models [12] as seen in figure 11. Crucially, this gives an extremely flexible family of distributions that ought to be able to capture the conditional structure that exists within a graph.

3.2.2 General Normalizing Flow Model

In general, the normalizing flow will will operate as follows:

1. A value will be sampled from a base distribution $b \sim \mathcal{B}$ with \mathcal{B} being a fixed base

distribution. In this case, we chose

$$\mathcal{B} = \text{Beta}(0.95, 0.95)$$

in order to bias the explanation towards sparse explanations that are favored in the literature [17].

2. The value then gets put through a series of m linear rational spline coupling normalizing flows giving the edge mask distribution. Let all the layers be denoted by $\mathcal{L}_{\mathcal{B}, \Theta}$ where Θ represents the parameters of the LRS layers. Therefore, we have

$$W_i = \sigma(\mathcal{L}_{\mathcal{B}, \Theta}(b))$$

where σ is the standard sigmoid function.

3. Finally, we get the conditional GNN classifier \hat{y} as the distribution given by

$$\hat{y} = \phi(v_i, \mathcal{X}, \mathcal{N}_l(v_i, E), W_i)$$

from which we apply a learning algorithm to obtain the weights Θ

4. Once this is done, the final edge interpretation is given by

$$\mathcal{W}_i = \mathbb{E}[\sigma(\mathcal{L}_{\mathcal{B}, \Theta})]$$

which is obtained simply by averaging Monte-Carlo sampling of the LRS layers.

For the graph edge interpretation model, this is the most general Bayesian algorithm that can be given due to the universality of the LRS coupling normalizing flow. Since the graph interpretation is expected to be quite a complicated distribution, the goal of this method is to capture all of the higher order complexities, including multi-hop relationships. The listing 2 succinctly captures this algorithm.

3.2.3 KL-Divergence and Direct Optimization

The first method used to train the parameters Θ is taking the distribution \hat{c} and c and backpropagating against the KL-divergence of these two distributions. Because of the reparametrization trick and the fact that the GNN is fully differentiable, this gives the gradient of the KL-divergence against Θ and allows for direct optimization against these parameters. Any SGD algorithm can be used, and, in particular, the ADAM optimizer [10] is used in this model.

Algorithm 2 The model setup for the Normalizing Flow model

Require: $v_i \in V, \bar{\alpha} > 0, \bar{\beta} > 0$ **Require:** $c \sim \phi(v_i, \mathcal{X}, \mathcal{N}_l(v_i, E), \mathcal{W})$ $b \sim B$ $W_i \leftarrow \sigma(\mathcal{L}_{\mathcal{B}, \Theta}(b))$ $\hat{y} \leftarrow \phi(v_i, \mathcal{X}, \mathcal{N}_l(v_i, E), W_i)$ $\hat{c} \sim \hat{y}$

3.2.4 ELBO and SVI

The second method is to use the ELBO and SVI method that was discussed before. Because the distributions in this model have already been reparametrized, there is no real major difference other than the stability of the training process. As such, this method is included for completeness even though, it is expected, that these two methods have the same theoretical outcome.

4 Experimental Setup

As was discussed in §2.1.1, there are many issues with the benchmarks that were proposed by [17]. Therefore, a major goal of this work was to confirm the intuition that these benchmarks were off. Then, the aim was to create a new set of benchmarks against which GNN interpretation models can be tested against. In this section, the methodology of these experiments will be walked through.

4.1 Validation of Incorrectness in Benchmark Datasets

4.2 Noise Filtering Experiment

4.3 Tree Embedding Experiment

5 Results

6 Discussion

References

- [1] Eunjoon Cho, Seth A. Myers, and Jure Leskovec. Friendship and mobility: user movement in location-based social networks. In *Proceedings of the 17th ACM SIGKDD international conference on Knowledge discovery and data mining*, KDD '11, pages 1082–1090. Association for Computing Machinery.
- [2] Takashi Washio and Hiroshi Motoda. State of the art of graph-based data mining. 5(1):59–68.
- [3] Francesca Petralia, Won-Min Song, Zhidong Tu, and Pei Wang. New method for joint network analysis reveals common and different coexpression patterns among genes and proteins in breast cancer. 15(3):743–754.
- [4] Rex Ying, Dylan Bourgeois, Jiaxuan You, Marinka Zitnik, and Jure Leskovec. GNNExplainer: Generating explanations for graph neural networks.
- [5] Michaël Defferrard, Xavier Bresson, and Pierre Vandergheynst. Convolutional neural networks on graphs with fast localized spectral filtering.
- [6] Thomas N. Kipf and Max Welling. Semi-supervised classification with graph convolutional networks.

- [7] Laurent Valentin Jospin, Wray Buntine, Farid Boussaid, Hamid Laga, and Mohammed Benamoun. Hands-on bayesian neural networks – a tutorial for deep learning users. 17(2):29–48.
- [8] Michael Betancourt. A conceptual introduction to hamiltonian monte carlo.
- [9] Matthew D. Hoffman and Andrew Gelman. The no-u-turn sampler: Adaptively setting path lengths in hamiltonian monte carlo.
- [10] Diederik P. Kingma and Jimmy Ba. Adam: A method for stochastic optimization.
- [11] Diederik P. Kingma and Max Welling. An introduction to variational autoencoders. 12(4):307–392.
- [12] Ivan Kobyzev, Simon J. D. Prince, and Marcus A. Brubaker. Normalizing flows: An introduction and review of current methods. 43(11):3964–3979.
- [13] Lilian Weng. Flow-based deep generative models. Section: posts.
- [14] Bing Xu, Naiyan Wang, Tianqi Chen, and Mu Li. Empirical evaluation of rectified activations in convolutional network.
- [15] Conor Durkan, Artur Bekasov, Iain Murray, and George Papamakarios. Neural spline flows.
- [16] Dongsheng Luo, Wei Cheng, Dongkuan Xu, Wenchao Yu, Bo Zong, Haifeng Chen, and Xiang Zhang. Parameterized explainer for graph neural network.
- [17] Hao Yuan, Haiyang Yu, Jie Wang, Kang Li, and Shuiwang Ji. On explainability of graph neural networks via subgraph explorations.
- [18] Wanyu Lin, Hao Lan, and Baochun Li. Generative causal explanations for graph neural networks.
- [19] Payam Dibaeinia and Saurabh Sinha. SERGIO: A single-cell expression simulator guided by gene regulatory networks. 11(3):252–271.e11.
- [20] E. N. Gilbert. Random graphs. 30(4):1141–1144. Publisher: Institute of Mathematical Statistics.
- [21] Eli Bingham, Jonathan P. Chen, Martin Jankowiak, Fritz Obermeyer, Neeraj Pradhan, Theofanis Karaletsos, Rohit Singh, Paul Szerlip, Paul Horsfall, and Noah D. Goodman. Pyro: Deep universal probabilistic programming.
- [22] Matthias Fey and Jan Eric Lenssen. Fast graph representation learning with PyTorch geometric.

- [23] Adam Paszke, Sam Gross, Francisco Massa, Adam Lerer, James Bradbury, Gregory Chanan, Trevor Killeen, Zeming Lin, Natalia Gimelshein, Luca Antiga, Alban Desmaison, Andreas Köpf, Edward Yang, Zach DeVito, Martin Raison, Alykhan Tejani, Sasank Chilamkurthy, Benoit Steiner, Lu Fang, Junjie Bai, and Soumith Chintala. PyTorch: An imperative style, high-performance deep learning library.
- [24] Continuous univariate distributions, volume 2, 2nd edition | wiley.
- [25] Marianna Bolla, Ahmed Elbanna, and Jozsef Mala. Estimating parameters of a directed weighted graph model with beta-distributed edge-weights.
- [26] Hadi M. Dolatabadi, Sarah Erfani, and Christopher Leckie. Invertible generative modeling using linear rational splines.

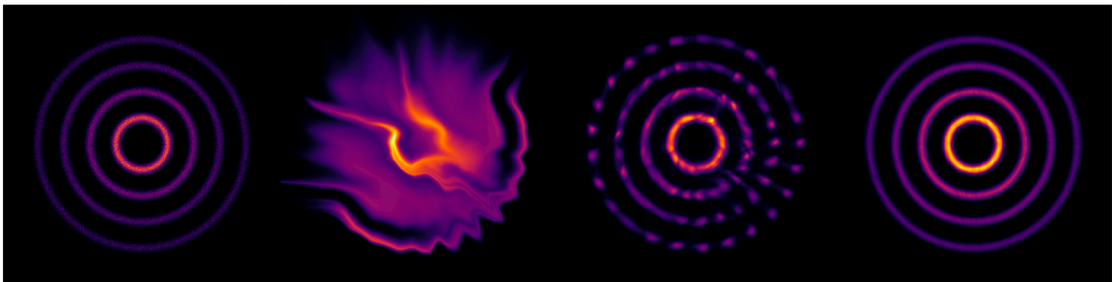


Figure 11: Different normalizing flow models on a synthetic conditionally distributed dataset. From left to right: ground truth, Glow, i-ResNet, Linear Rational Splines (this method). Taken from [26]